

Intermittent Single-Molecule Interfacial Electron Transfer Dynamics

Vasudevanpillai Biju, Miodrag Micic,[†] Dehong Hu, and H. Peter Lu*

Contribution from the Pacific Northwest National Laboratory, Fundamental Science Division,
P. O. Box 999, Richland, Washington 99352

Received February 17, 2004; Revised Manuscript Received May 10, 2004; E-mail: peter.lu@pnl.gov

Abstract: We report on single-molecule studies of photosensitized interfacial electron transfer (ET) processes in Coumarin 343 (C343)–TiO₂ nanoparticles (NP) and Cresyl Violet (CV⁺)–TiO₂ NP systems, using time-correlated single-photon counting coupled with scanning confocal fluorescence microscopy. Fluorescence intensity trajectories of individual dye molecules adsorbed on a semiconductor NP surface showed fluorescence fluctuations and blinking, with time constants distributed from milliseconds to seconds. The fluorescence fluctuation dynamics were found to be inhomogeneous from molecule to molecule and from time to time, showing significant static and dynamic disorders in the interfacial ET reaction dynamics. We attribute fluorescence fluctuations to the interfacial ET reaction rate fluctuations, associating redox reactivity intermittency with the fluctuations of molecule–TiO₂ electronic and Franck–Condon coupling. Intermittent interfacial ET dynamics of individual molecules could be characteristic of a surface chemical reaction strongly involved with and regulated by molecule–surface interactions. The intermittent interfacial reaction dynamics that likely occur among single molecules in other interfacial and surface chemical processes can typically be observed by single-molecule studies but not by conventional ensemble-averaged experiments.

Introduction

Interfacial electron transfer (ET) processes play an important role in many chemical and biological processes. Specifically, interfacial ET in TiO₂-based systems has been used in artificial solar energy harvesting^{1–9} and in wastewater catalytic and advanced oxidative treatments.^{4,7,8,10–15} The fundamental importance and impending applications make the study of inter-

facial ET a promising research area.^{1–8,10–53} Using ultrafast spectroscopy and ensemble-averaging approaches, the dynamics of the ET processes have been studied and the presence of

[†] Present address: M P Biomedicals Inc., 15 Morgan, Irvine, CA 93618.

- (1) Fujishima, A.; Honda, K. *Nature* **1972**, *238*, 37–38.
- (2) O'Regan, B.; Grätzel, M. *Nature* **1991**, *353*, 737–740.
- (3) Hagfeldt, A.; Björkstén, U.; Grätzel, M. *J. Phys. Chem.* **1996**, *100*, 8045–8048.
- (4) Wu, T.; Liu, G.; Zhao, J.; Hidaka, H.; Serpone, N. *J. Phys. Chem. B* **1999**, *103*, 4862–4867.
- (5) Grätzel, M. *Nature* **2001**, *414*, 338–344.
- (6) Bauer, C.; Boschloo, G.; Mukhtar, E.; Hagfeldt, A. *J. Phys. Chem. B* **2002**, *106*, 12693–12704.
- (7) Bisquert, J.; Zaban, A.; Salvador, P. *J. Phys. Chem. B* **2002**, *106*, 8774–8782.
- (8) Fox, M. A.; Dulay, M. T. *Chem. Rev.* **1993**, *93*, 341–357.
- (9) Adams, D. M.; Brus, L.; Chidsey, C. E. D.; Creager, S.; Creutz, C.; Kagan, C. R.; Kamat, P. V.; Lieberman, M.; Lindsay, S.; Marcus, R. A.; Metzger, R. M.; Michel-Beyerle, M. E.; Miller, J. R.; Newton, M. D.; Rolison, D. R.; Sankey, O.; Schanze, K. S.; Yardley, J.; Zhu, X. Y. *J. Phys. Chem. B* **2003**, *107*, 6668–6697.
- (10) Kamat, P. V.; Huehn, R.; Nicolaescu, R. *J. Phys. Chem. B* **2002**, *106*, 788–784.
- (11) Gray, K. A.; Stafford, U.; Dieckmann, M. S.; Kamat, P. V. *Mechanistic studies in TiO₂ systems: Photocatalytic degradation of chloro- and nitrophenols, in Photocatalytic Purification and Treatment of Water and Air*; Ollis, D. F., Al-Ekabi, H., Eds.; Elsevier Science: Amsterdam 1993; pp 8–13.
- (12) Linsebigler, A. L.; Lu, G.; Yates, J. T. *Chem. Rev.* **1995**, *95*, 735–758.
- (13) Stock, N. L.; Peller, J.; Vinodgopal, K.; Kamat, P. V. *Environ. Sci. Technol.* **2000**, *34*, 1747–1750.
- (14) Serpone, N. *Res. Chem. Intermed.* **1994**, *20*, 953–992.
- (15) Liu, G.; Wu, T.; Zhao, J.; Hidaka, H.; Serpone, N. *Environ. Sci. Technol.* **1999**, *33*, 2081–2087.
- (16) Asbury, J. B.; Hao, E.; Wang, Y. Q.; Ghosh, H. N.; Lian, T. Q. *J. Phys. Chem. B* **2001**, *105*, 4545–4557.
- (17) Brown, G. T.; Darwent, J. R.; Fletcher, P. D. I. *J. Am. Chem. Soc.* **1985**, *107*, 6446–6451.
- (18) Burfeindt, B.; Hannappel, T.; Storck, W.; Willig, F. *J. Phys. Chem.* **1996**, *100*, 16463–16465.
- (19) Duonghong, D.; Ramsden, J.; Grätzel, M. *J. Am. Chem. Soc.* **1982**, *104*, 2977–2985.
- (20) Durrant, J. R. *J. Photochem. Photobiol., A* **2002**, *148*, 5–10.
- (21) Gaal, D. A.; Hupp, J. T. Photoinduced electron-transfer reactivity at nanoscale semiconductor/solution interfaces: Case studies with dye sensitized SnO₂/water surfaces; In *Molecular and supramolecular photochemistry*; Schanze, K. S., Ramamurthy, V., Eds.; Marcel Dekker: New York, 2003; Vol. 10, pp 89–121.
- (22) Ghosh, H. N. *J. Phys. Chem. B* **1999**, *103*, 10382–10387.
- (23) Ghosh, H. N.; Asbury, J. B.; Weng, Y. X.; Lian, T. Q. *J. Phys. Chem. B* **1998**, *102*, 10208–10215.
- (24) Hao, E.; Anderson, N. A.; Asbury, J. B.; Lian, T. *J. Phys. Chem. B* **2002**, *106*, 10191–10198.
- (25) Haque, S. A.; Tachibana, Y.; Klug, D. R.; Durrant, J. R. *J. Phys. Chem. B* **1998**, *102*, 1745–1749.
- (26) Holman, M. W.; Liu, R.; Adams, D. A. *J. Am. Chem. Soc.* **2003**, *125*, 12649–12654.
- (27) Huang, S. Y.; Schlichthörl, G.; Nozik, A. J.; Grätzel, M.; Frank, A. J. *J. Phys. Chem. B* **1997**, *101*, 2576–2582.
- (28) Huber, R.; Moser, J. E.; Grätzel, M.; Wachtveitl, J. *Chem. Phys.* **2002**, *285*, 39–45.
- (29) Iwai, S.; Hara, K.; Murata, S.; Katoh, R.; Sugihara, H.; Arakawa, H. *J. Phys. Chem.* **2000**, *113*, 3366–3373.
- (30) Grätzel, M. *Heterogeneous Photochemical Electron Transfer*; CRC Press, Inc.: Boca Raton, FL, 1987.
- (31) Kamat, P. V. Electron-transfer processes in nanostructured semiconductor thin films; In *Nanoparticles and nanostructural films*; Fendler, J., Ed.; Wiley-VCH: New York, 1998.
- (32) Kamat, P. V. *J. Phys. Chem. B* **2002**, *106*, 7729–7744.
- (33) Lemon, B. I.; Hupp, J. T. *J. Phys. Chem. B* **1999**, *103*, 3797–3799.
- (34) Liu, D.; Fessenden, R. W.; Hug, G. L.; Kamat, P. V. *J. Phys. Chem. B* **1997**, *101*, 2583–2590.

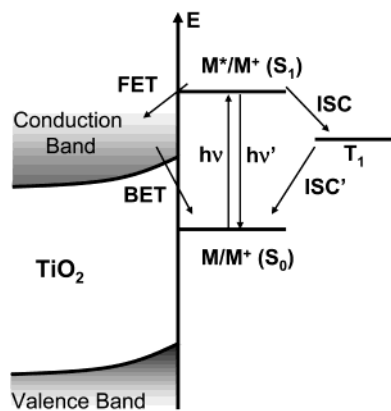


Figure 1. Schematic presentation of a model of photoinduced processes in a dye-sensitized TiO₂ system.

inhomogeneities in the interfacial ET dynamics has been revealed. However, significant questions remain on characterizing the inhomogeneities.^{16,18,20,22–29,34,35,37,40,42–46,48} Photoexcitation of dye molecules adsorbed on the surface of wide band gap semiconductors such as TiO₂ and SnO₂ result in the injection of electrons from the dye molecules to the conduction band of the semiconductor or energetically accessible surface electronic states.^{10–12,16–37,40–49,54} A general model of photoinduced processes in a dye-sensitized semiconductor system may be represented as in Figure 1. The forward electron transfer (FET) kinetics in various dye–TiO₂ ET systems are nonexponential, with half-times disseminated in the femtoseconds to several hundred picoseconds range.^{16,18–20,23,24,28,29,36,42–46,48} Following the FET, the thermalized injected electron is localized to either subband states or surface states of the TiO₂ semiconductor.^{8,16,20,24,25,29,40,44,46,48,55} Typically, a backward electron transfer (BET) from the semiconductor to the oxidized dye molecules will follow.^{19,20,22–28,34,40–42,45,48} In interfacial ET systems, a BET process is possible by thermal detrapping of the electrons from the total electron density of the reduced semiconductor and recombining the electrons with the oxidized dye molecules.²⁰ Compared to ultrafast FET processes, BET

processes take place on a longer time scale, ranging from subnanoseconds to several milliseconds, probably due to the existence of trap states and non-Brownian diffusion motions of the electrons in semiconductors. Furthermore, the dynamics of the BET processes are often nonexponential or stretched-exponential.^{19,20,22–28,34,40–42,45,48} Designing an efficient solar energy harvesting system entails controlling the rate of the BET process in order to generate long-lived charge-separated states. Characterizations of the electron trap states and localized subband states are important because these states play a regulating role on inhomogeneous BET dynamics and, in turn, the fluorescence dark-state lifetimes of the oxidized dye molecules.

The inhomogeneous nanoscale molecule–surface and molecule–molecule interactions are presumably the origins of the complexity in interfacial ET dynamics. These nanoscale inhomogeneities at interfaces or on surfaces make it highly difficult for ensemble-averaged measurements to dissect the complex interfacial ET processes, which, from time to time, have produced different experimental results, such as the reported rate constants^{16,18–20,23,24,26,28,29,36,42–46,48,56} of FET and BET. The difficulty comes from both spatial and temporal inhomogeneities, which can be identified, measured, and analyzed best by studying one molecule at a time in a specific nanoscale local environment.

Single-molecule spectroscopy has been demonstrated to be a powerful approach for studying complex systems and inhomogeneous dynamics^{57–65} and has also been applied to intramolecular⁵⁶ and interfacial ET investigations.^{26,37} To account for the inhomogeneous rates of the ET that originate from intrinsic complex dynamic reaction processes, we studied the dynamics of interfacial ET processes of individual dye molecules adsorbed on the surface of TiO₂ nanoparticles (NPs). With single-molecule spectroscopy, this study of interfacial ET dynamics of individual molecules avoided interference from (i) molecular aggregation, (ii) multiple electron injection to a single particle, and (iii) multiple electron–cation recombinations on the surface of a single particle.

For modeling interfacial ET systems, we chose to study Coumarin 343 (C343)–TiO₂ NP and Cresyl Violet (CV⁺)–TiO₂ NP systems. These systems exhibit a number of amenable properties for such research: (i) since a TiO₂ semiconductor is an essential substrate in many solar cells, interfacial ET processes in dye–TiO₂ NP systems have a potential industrial importance;^{1–8} (ii) the high fluorescence quantum efficiencies of C343 ($\Phi_f = \sim 0.7$)²⁴ and CV⁺ ($\Phi_f = \sim 0.545$)⁶⁶ make it feasible to use single-molecule fluorescence spectroscopy to study interfacial ET processes; (iii) it has already been dem-

(35) Liu, D.; Kamat, P. V. *J. Phys. Chem.* **1996**, *100*, 965–970.

(36) Lu, H.; Prieskorn, J. N.; Hupp, J. T. *J. Am. Chem. Soc.* **1993**, *115*, 4927–4928.

(37) Lu, H. P.; Xie, X. S. *J. Phys. Chem. B* **1997**, *101*, 2753–2757.

(38) Marcus, R. A. *J. Chem. Phys.* **1956**, *24*, 966–978.

(39) Marcus, R. A. *Annu. Rev. Phys. Chem.* **1964**, *15*, 155–196.

(40) Miller, R. J. D.; McLendon, G. L.; Nozik, A.; Schmickler, W.; Willig, F. *Surface Electron-Transfer Processes*; Wiley-VCH: New York, 1995.

(41) O'Regan, B.; Moser, J.; Anderson, M.; Grätzel, M. *J. Phys. Chem.* **1990**, *94*, 8720–8726.

(42) Pan, J.; Benkő, G.; Xu, Y.; Pascher, T.; Sun, L.; Sundström, V.; Polívka, T. *J. Am. Chem. Soc.* **2002**, *124*, 13949–13957.

(43) Pelet, S.; Grätzel, M.; Moser, J. E. *J. Phys. Chem. B* **2003**, *107*, 3215–3224.

(44) Ramakrishna, G.; Ghosh, H. N. *J. Phys. Chem. A* **2002**, *106*, 2545–2553.

(45) Tachibana, Y.; Moser, J. E.; Grätzel, M.; Klug, D. R.; Durrant, J. R. *J. Phys. Chem.* **1996**, *100*, 20056–20062.

(46) Tachibana, Y.; Rubstov, I. V.; Montanari, I.; Yoshihara, K.; Klug, D. R.; Durrant, J. R. *J. Photochem. Photobiol., A* **2001**, *142*, 215–220.

(47) Walters, K. A.; Gaal, D. A.; Hupp, J. T. *J. Phys. Chem. B* **2002**, *106*, 5139–5142.

(48) Willig, F.; Zimmermann, C.; Ramakrishna, S.; Storck, W. *Electrochim. Acta* **2000**, *45*, 4565–4575.

(49) Yan, S. G.; Hupp, J. T. *J. Phys. Chem. B* **1997**, *101*, 1493–1495.

(50) Hoffmann, R.; Imamura, A.; Hehre, W. J. *J. Am. Chem. Soc.* **1968**, *90*, 1499–1509.

(51) Kavarnos, G. J.; Turro, N. J. *Chem. Rev.* **1986**, *86*, 401–449.

(52) Newton, M. D. *Chem. Rev.* **1991**, *91*, 767–792.

(53) Paddon-Row, M. N. *Acc. Chem. Res.* **1982**, *15*, 245–251.

(54) Yu, J.; Chen, J.; Wang, X.; Zhang, B.; Cao, Y. *Chem. Commun.* **2003**, 1856–1857.

(55) Colombo, D. P.; Browman, R. M. *J. Phys. Chem.* **1995**, *99*, 11752–11756.

(56) Liu, R.; Holman, M.; Zang, L.; Adams, D. M. *J. Phys. Chem. A* **2003**, *107*, 6522–6526.

(57) Betzig, E.; Chichester, R. J. *Science* **1993**, *262*, 1422–1425.

(58) Trautman, J. K.; Macklin, J. J.; Brus, L. E.; Betzig, E. *Nature* **1994**, *369*, 40–42.

(59) Xie, X. S. *Acc. Chem. Res.* **1996**, *29*, 598–606.

(60) Xie, X. S.; Dunn, R. C. *Science* **1994**, *265*, 361–364.

(61) vanden Bout, D. A.; Yip, W. T.; Hu, D. H.; Fu, D. K.; Swager, T. M.; Barbara, P. F. *Science* **1997**, *277*, 1074–1077.

(62) Macklin, J. J.; Trautman, J. K.; Harris, T. D.; Brus, L. E. *Science* **1996**, *272*, 255–258.

(63) Lu, H. P.; Xie, X. S. *Nature* **1997**, *385*, 143–146.

(64) Biju, V.; Ye, J. Y.; Ishikawa, M. *J. Phys. Chem. B* **2003**, *107*, 10729–10735.

(65) Hu, D. H.; Yu, J.; Barbara, P. F. *J. Am. Chem. Soc.* **1999**, *121*, 6936–6937.

(66) Magde, D.; Brannon, J. H.; Cremers, T. L.; Olmsted, J., III. *J. Phys. Chem.* **1979**, *83*, 696–699.

onstrated that C343^{22,24,28,44} and CV^{+34,35,37,67,68} adsorbed on semiconductor surfaces are efficient electron donors under photoexcitation; (iv) the systems can be used to validate single-molecule spectroscopy as a way to study interfacial ET processes involving chromophores that absorb in the near-UV (C343) and visible region (CV⁺); and (v) the oxidized dye molecules have different charge densities, +2 charges on CV and +1 charge on C343, making them an informative comparison. Interfacial ET processes involving C343 have been explicitly proven by probing the ultrafast ET processes and ET products (cation radical of C343 and trapped electron in TiO₂ colloidal particles) in thorough ensemble-averaged studies of the TiO₂–C343 system.^{22,24,28,44,69} Interfacial ET processes involving monomers or aggregates of CV⁺ as electron donor have been reported in a previous single-molecule ET study³⁷ and in other ensemble-averaged ET studies.^{34,35,37,67,68} Here, we report on interfacial ET dynamics of single molecules of C343 and CV⁺ adsorbed on TiO₂ NP surfaces. Having observed single-molecule fluorescence intensity fluctuations and blinking, we attribute these phenomena to intermittency^{70–73} of the interfacial ET processes.

Experimental Section

Materials and Methods. C343, titanium isopropoxide, poly(methyl methacrylate) (PMMA) (av MW = 12 000), acetone, and toluene were purchased from Aldrich, and Cresyl violet acetate was purchased from Exciton Inc.. All the reagents were used as supplied. Cover slips (Fisher) were thoroughly cleaned by sonication in aqueous NaOH solution (0.1 M), deionized water, acetone, and deionized water, respectively, each for 15 min and dried in a jet of nitrogen gas. Nanometer-size TiO₂ particles were prepared by the hydrolysis of titanium isopropoxide.⁷⁴ Single-molecule control samples were prepared by first spin-coating a 25 μ L, 0.1 nM aqueous solution of a dye (C343 or CV⁺) on a clean cover slip at 3000 rpm, followed by overlaying a PMMA film by spin-coating a 50 μ L toluene solution of PMMA (1 mg/mL) at 3000 rpm. Samples for the study of single-molecule ET processes were prepared by first spin-coating a 50 μ L dilute solution of TiO₂ NPs (containing \sim 0.8 μ M TiO₂) on a cover slip at 3000 rpm, followed by spin-coating a 0.1 nM (25 μ L) aqueous solution of a dye (C343 or CV⁺). Finally, the dye molecules were covered using an overlayer of PMMA produced by spin-coating a 50 μ L toluene solution of PMMA (1 mg/mL). TiO₂ NP samples for atomic force microscopy (AFM) were prepared by spin-coating a 50 μ L stock TiO₂ NP solution.

Characterization of the TiO₂ NPs. We characterized the phase and the size of TiO₂ NPs using transmission electron microscopy (TEM) and AFM imaging. TEM images show crystal lattice fringes, characteristic of the Anatase phase of TiO₂ NPs (Figure 2A). Characterization of the size of the NPs was made using AFM tapping-mode imaging in air (Figure 2B and C). Figure 2B shows a high density of TiO₂ NPs on a cover glass surface. The samples prepared under essentially the same coverage of TiO₂ nanoparticles were used in the single-molecule ET dynamics studies in this work. The size and size distributions of the NPs are more clearly represented in an AFM image (Figure 2C) of a sample prepared by spin-coating a 20-times diluted TiO₂ NP colloidal solution on a mica surface. The sizes of TiO₂ NPs, based on the height measurements by AFM, ranged from 6 to 15 nm.

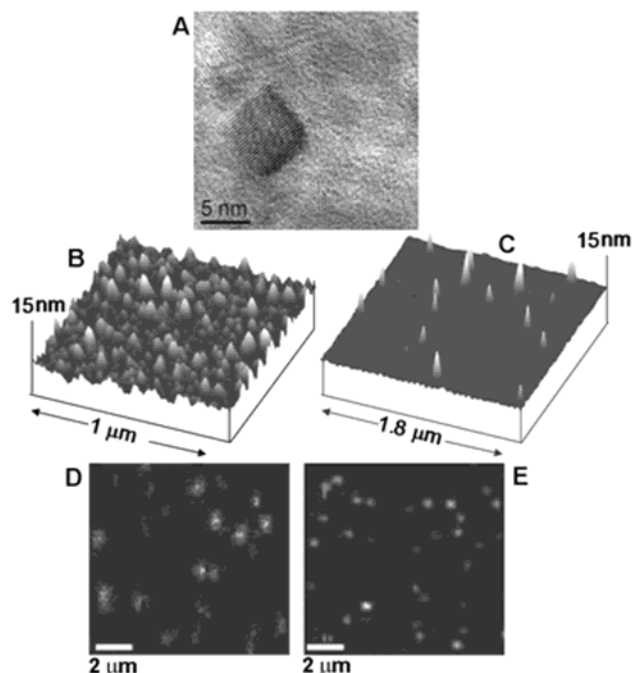


Figure 2. A high-resolution TEM image of TiO₂ NPs obtained under 300 kV acceleration and 600 k magnification (A). AFM images obtained for a 0.8 μ M colloidal TiO₂ NP solution spin-coated on a cover glass slip (B) (samples prepared under this condition were overcoated with C343 or CV⁺ dye molecules and used in single-molecule fluorescence studies) and a 40 nM colloidal TiO₂ NP solution spin-coated on a freshly cleaved mica surface (C). Fluorescence images of single molecules of C343 (D) and CV⁺ (E) spin-coated on TiO₂ NP coated cover glass slips (topographies of these samples are identical to those in B). The scale bar in image A is 5 nm, and those in images D and E are 2 μ m.

Single-Molecule Fluorescence Spectroscopy and Imaging. We studied the single-molecule interfacial ET dynamics of C343–TiO₂ NP and CV⁺–TiO₂ NP systems by probing the single-molecule fluorescence intensity time trajectories. Single-molecule fluorescence images and fluorescence intensity trajectories were recorded using a Zeiss inverted sample-scanning confocal microscope, equipped with a 100 \times 1.3 NA oil immersion objective (Zeiss FLUAR), single-photon-counting avalanche photodiode (APD) detector (Perkin-Elmer SPCM-AQR-15), homemade photon time-stamping electronics,⁷⁵ and scanning piezo-electric stage (QI NPS 3330, Queensgate Instruments, Berkshire, England). Experiments in an inert atmosphere were carried out under a controlled flow of N₂ gas using a flow controller (A55496-Harvard Apparatus, MA). A 568 nm cw Krypton laser (Coherent Innova) was used for exciting CV⁺ molecules, and C343 molecules were excited using a 441.6 nm cw HeCd laser (Linconix). Excitation power used for imaging was 500 nW, and that for trajectory recording was 250 nW.

The transition dipole orientations of single molecules^{57,61,76–83} were determined by analyzing fluorescence intensity trajectories, which were recorded upon a modulated linear polarized laser excitation. In these

(67) Parkinson, B. A.; Spitzer, M. T. *Electrochim. Acta* **1992**, *37*, 943–948.
 (68) Kietzmann, R.; Willig, F.; Weller, H.; Vogel, R.; Nath, D. N.; Eichberger, R.; Liska, P.; Lehnert, J. *Mol. Cryst. Liq. Cryst.* **1991**, *194*, 169–180.
 (69) Leytner, S.; Hupp, J. T. *Chem. Phys. Lett.* **2000**, *330*, 231–236.
 (70) Wang, J.; Wolyne, P. *Phys. Rev. Lett.* **1995**, *74*, 4317–4320.
 (71) Jung, Y. J.; Barkai, E.; Silbey, R. J. *Chem. Phys.* **2003**, *284*, 181–194.
 (72) Toniolo, C.; Provenzale, A.; Spiegel, E. A. *Phys. Rev. E* **2002**, *66*, 066209-1-12.
 (73) Xie, X. S. *J. Chem. Phys.* **2002**, *117*, 11024–11032.
 (74) Duonghong, D.; Borgarello, E.; Grätzel, M. *J. Am. Chem. Soc.* **1981**, *103*, 4685–4690.

(75) Hu, D. H.; Lu, H. P. *J. Phys. Chem. B* **2003**, *107*, 618–626.
 (76) Guttler, F.; Croci, M.; Renn, A.; Wild, U. P. *Chem. Phys.* **1996**, *211*, 421–430.
 (77) Bloess, A.; Durand, Y.; Matsushita, M.; Schmidt, J.; Groenen, E. J. *J. Chem. Phys. Lett.* **2001**, *344*, 55–60.
 (78) Ha, T.; Laurence, T. A.; Chemla, D. S.; Weiss, S. J. *Phys. Chem. B* **1999**, *103*, 6839–6850.
 (79) Sick, B.; Hecht, B.; Novotny, L. *Phys. Rev. Lett.* **2000**, *85*, 4482–4485.
 (80) Sepiol, J.; Jasny, J.; Keller, J.; Wild, U. P. *Chem. Phys. Lett.* **1997**, *273*, 444–448.
 (81) Dickson, R. M.; Norris, D. J.; Moerner, W. E. *Phys. Rev. Lett.* **1998**, *81*, 5322–5325.
 (82) Bartko, A. P.; Xu, K. W.; Dickson, R. M. *Phys. Rev. Lett.* **2002**, *89*, 026101-1-4.
 (83) Vacha, M.; Kotani, M. *J. Chem. Phys.* **2003**, *118*, 5279–5282.

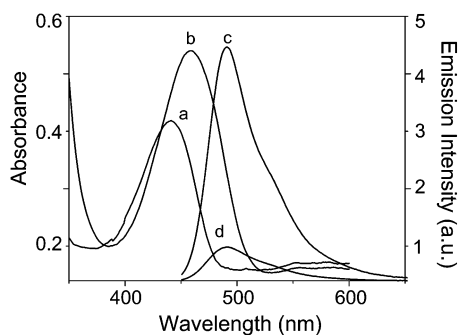


Figure 3. Steady-state absorption and emission spectra of methanol solutions of C343: (A and B) absorption spectra in the absence and in the presence ($\sim 10 \mu\text{M}$) of TiO_2 NPs, respectively; (C and D) emission spectra in the absence and in the presence ($\sim 10 \mu\text{M}$) of TiO_2 NPs, respectively. The red-shift in the absorption spectrum is due to charge-transfer interactions, and fluorescence quenching is due to interfacial ET.

measurements, a combination of an electro-optical modulator (Laser-matrix 3079.6, Fast-Pulse Technology, NJ) and a quarter wave plate was used to change the excitation polarization. The linear polarized laser was passed through the electro-optical modulator, and the polarization was rotated at 1 kHz using a voltage controller (ConOptics 302, Danbury, CT).

Solutions ($25 \mu\text{L}$, 0.1 nM) of the dye molecules were spin-coated on a glass surface or on a TiO_2 NP coated glass surface and covered using a thin film of PMMA to protect the dye molecules from oxygen-associated photobleaching. Fluorescence images (Figure 2D and E) of single molecules of C343 and CV^+ on a TiO_2 NP coated glass surface were obtained by raster-scanning the samples over a focused laser spot of $\sim 300 \text{ nm}$ diameter. Discrete fluorescence spots in Figure 2D and E were attributed to single dye molecules, based on irreversible photobleaching in a single step and by identifying the polarized emissions. A higher background emission was observed for C343– TiO_2 NP samples while using a 441.6 nm excitation as compared to that from CV^+ – TiO_2 samples excited at 568 nm . Single-molecule fluorescence images from C343– TiO_2 NP samples typically produced a lower contrast, which is likely due to the excitation at 441.6 nm generating a higher background emission from TiO_2 NP because the excitation is close to the band gap excitation at $\sim 3.2 \text{ eV}$.

Results and Discussion

We examined the absorption and emission properties of C343 and CV^+ dye molecules in solutions and in the presence of electron-accepting TiO_2 NPs. Figure 3 shows absorption (trace a) and emission (trace c) spectrums of C343 dye solutions in the absence and in the presence of TiO_2 NPs.

The absorption band of C343 dye shows a red shift of $\sim 20 \text{ nm}$ in the presence of TiO_2 NPs (trace b in Figure 3). Furthermore, the fluorescence of C343 dye solution is considerably quenched in the presence of TiO_2 NPs (trace d in Figure 3). The red shift in the absorption and the fluorescence quenching are consistent with the literature and have been attributed, respectively, to charge transfer (CT) and ET interactions between the dye molecules and TiO_2 NPs.^{22,28,34,36} The time scales of the FET and BET processes have been reported to be from femtoseconds to subnanoseconds and from picoseconds to sub-milliseconds, respectively.^{22,24,28,44} Similar absorption and emission properties are observed for CV^+ molecules in the presence of TiO_2 NPs, although the effects are less predominant compared to those of the C343– TiO_2 NP system.

We examined the single-molecule interfacial ET processes by recording and analyzing the fluorescence intensity trajectories of individual C343 and CV^+ molecules adsorbed on the surface

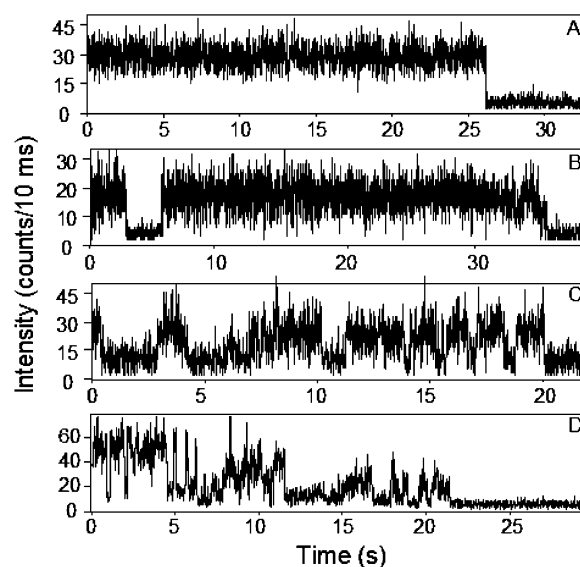


Figure 4. Fluorescence intensity trajectories collected in air for single molecules of C343 or CV^+ , with samples prepared by spin-coating aqueous dye solutions (0.1 nM) on cover glass slips or on TiO_2 NP coated cover glass slips and overlaid with a thin film of PMMA: (A) trajectory of C343 in the absence of TiO_2 NP; (B and C) trajectories of C343 in the presence of TiO_2 NPs; and (D) trajectory of CV^+ in the presence of TiO_2 NPs. The binning time for the trajectories was 10 ms . The fluorescence fluctuation characteristics observed (B–D) are due to intermittent interfacial ET reactivity.

of TiO_2 NPs. In our experiments, a thin layer of TiO_2 NPs was spin-coated on a glass cover slip (Figure 2B), followed by spin-coating a solution (0.1 nM) of C343 or CV^+ . The dye molecules were covered using a thin film of PMMA by spin-coating a toluene solution of PMMA (1 mg/mL). Fluorescence intensity trajectories of C343 and CV^+ single molecules adsorbed on bare glass surfaces and on the surfaces of TiO_2 NPs were measured by single-photon time-stamping.⁷⁵ Uninterrupted fluorescence states, i.e., no fluorescence blinking or fluctuation, were essentially observed for both C343 and CV^+ molecules in the absence of TiO_2 NPs on insulating glass surfaces. Figure 4A shows a typical fluorescence intensity trajectory of a single C343 molecule on a glass surface. Dye molecules at the singlet excited states exhibit different excited-state electronic deactivation processes: internal conversion, fluorescence emission, and intersystem crossing to a dark triplet state (Figure 1). Under ambient conditions and millisecond temporal resolutions, it is rare to observe fluorescence blinking of these molecules due to intersystem crossing to the dark triplet-state and ground-state recovery. These processes usually occur on a much shorter time scale; for example, quenching of the triplet state by oxygen is on a sub-millisecond time scale.⁸⁴ In our experiments, we used sub-millisecond temporal resolution for single-photon counting and a 10 ms bin time for recording and analyzing single-photon arrival time. These time scales allowed any fast fluorescence intensity fluctuations or blinking of the dye molecules to be averaged out within our measurements. On the other hand, we observed fast fluorescence blinking due to intersystem crossing to long-lived dark triplet states in a nitrogen atmosphere, using millisecond or shorter bin-time recording.

Typical fluorescence intensity trajectories obtained for two single C343 molecules, adsorbed on the surface of TiO_2 NPs

(84) Birks, J. B. *Organic Molecular Photophysics*; Wiley-VCH: New York, 1973.

and recorded in air, are shown in Figure 4B and C. Figure 4D shows a typical fluorescence intensity trajectory of a single CV⁺ molecule adsorbed on the surface of a TiO₂ NP and recorded in air. Under these conditions, fluorescence intensity trajectories of both C343 and CV⁺ single molecules showed fluctuation behavior. The single-molecule fluorescence intensities stochastically dropped to either a lower or background level. For both the C343 and CV⁺ single molecules, the time scales of fluorescence intensity fluctuations ranged from several milliseconds to several seconds and also the fluctuation behavior was found to differ among the single molecules.

Based on our experimental results and the literature, we are able to attribute the fluorescence intensity fluctuation behavior of single molecules adsorbed on TiO₂ NP surfaces to interfacial ET reactions for the following reasons: (i) the oxidized states of the dyes were essentially nonfluorescent, in contrast to their bright reduced forms;^{28,37} (ii) ensemble-averaged fluorescence and transient absorption studies have demonstrated that photoexcited C343 molecules inject electrons to the conduction band or energetically accessible surface states of the TiO₂ semiconductor,^{22,24,28,44} and both ensemble-averaged^{34,35,67,68} and single-molecule³⁷ studies have identified interfacial ET reactions of CV⁺ on semiconductor surfaces; (iii) fluorescence intensity trajectories of single molecules of C343 (Figure 4A) and CV⁺ (not shown) in the absence of TiO₂ NPs in our control experiments showed essentially continuous fluorescence until the molecules were irreversibly photobleached; (iv) ET between the dye molecules and a PMMA film is unlikely, based on our control experiment (Figure 4A), in which the dye molecules were directly deposited on a glass surface and followed by covering with a PMMA layer; and (v) the fluorescence intensity fluctuations were not due to triplet states or the rotation of the transition dipoles of the dye molecules (details are discussed below).

We have investigated the possibility that transient changes in the transition dipole orientations of the single molecules, as a result of molecular rotational or translational motions, are responsible for the observed fluorescence fluctuations and blinking in subseconds to seconds (Figure 4B–D). Dye molecules adsorbed on TiO₂ NP surfaces may change their orientations as a result of the collective motions of the molecular environment or rotational and translational motions of the dye molecules. Under linearly polarized laser excitation, changes in the excitation cross section due to changes in molecular orientation result in fluorescence intensity changes.^{61,64,65} In our single-molecule control experiments, we recorded single-molecule fluorescence intensity time trajectories using an orientation angle-modulated linear polarized laser excitation.

We determined the transition dipole orientation angles of single molecules by analyzing the fluorescence intensity trajectories. Figure 5A shows a typical intensity trajectory obtained for a single C343 molecule, adsorbed on a TiO₂ NP surface, under a 1 kHz rotationally modulated linear polarized 441.6 nm laser excitation. The trajectory shows deep sine-wave modulation, suggesting the fluorescence is from a single transition dipole, and the phase of the sine wave presents the orientation of the transition dipole. To determine the orientation changes of single-molecule transition dipoles, we analyzed the sine-wave modulation of the fluorescence intensity trajectories. In the fluorescence intensity trajectory of a single C343

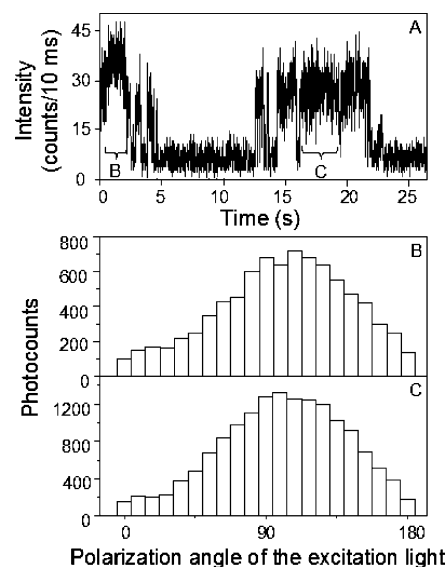


Figure 5. (A) Fluorescence intensity trajectory obtained for a single C343 molecule adsorbed on a TiO₂ NP surface under excitation, using a rotationally modulated (1 kHz) linear polarized 441.6 nm laser beam. The transition dipole orientations of the single C343 molecule at two different time intervals are provided in parts B and C. The transition dipole orientations in parts B and C are determined from the photocounts collected in the trajectory (A) during 1.5–2.8 s and 17.5–20.5 s [see the open bracket indications in part A]. The constant nature of the transition dipole orientation rules out that change in the excitation cross section due to molecular rotation or translation is included in the fluorescence fluctuation behavior of single molecules.

molecule, the sine-wave modulation and phase obtained for two time intervals (Figure 5A) are the same (Figure 5B and C) within our measurement sensitivity (any change of dipole orientation >10°). More than 80% of the single-molecule fluorescence intensity trajectories show a constant sine-wave phase, which suggests that the transition dipole orientations of single molecules do not change significantly. However, the intensity fluctuates along the trajectory. These observations substantiate the conclusion that molecular rotation or translation is not primarily responsible for the fluorescence fluctuation and blinking in the intensity trajectories (Figures 4B–D, 5A).

Based on control experiments, we have ruled out a contribution from the dark triplet state to the fluorescence intensity fluctuations and blinking on a time scale longer than milliseconds. In the control experiments, single-molecule fluorescence trajectories showed no intensity fluctuation in the absence of TiO₂ NPs under ambient experimental conditions. It is known that, in an inert atmosphere, the triplet lifetime is substantially extended compared to that in the presence of strong triplet scavengers, such as oxygen.⁸⁴ We observed the fluorescence blinking of single molecules of C343 and CV⁺ in an inert atmosphere and in the absence of TiO₂ NPs on a millisecond time scale. We attribute this fluorescence blinking to transient trapping of the excited states in long-lived triplet states of the dye molecules. Figure 6A and D show single-molecule fluorescence intensity trajectories of C343 and CV⁺ molecules adsorbed on glass surfaces, followed by covering with PMMA films, and recorded under continuous nitrogen purging. A zoom-in portion of the trajectory shows stochastic fluorescent “on” and triplet “off” states of a single molecule (Figure 6B). Fluorescence blinking due to a dark triplet state is on a millisecond time scale, which is much faster than those in Figures 4B–D and 5A. We have characterized the triplet-state

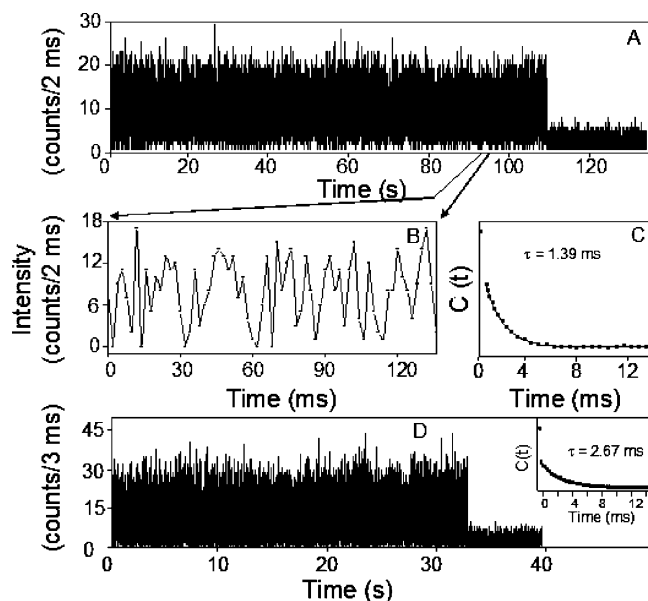


Figure 6. Fluorescence intensity trajectories obtained for single molecules of C343 (A) and CV⁺ (D) under nitrogen atmosphere, showing blinking due to intersystem crossing to long-lived dark triplet states. Trajectory details of blinking of a single C343 molecule are presented in a zoom-in trajectory (B). Single-exponential autocorrelation traces for the trajectories in part A and in part D are provided, respectively, in part C and in the inset of part D.

blinking dynamics by analyzing the autocorrelation functions, calculated from the single-molecule trajectories (Figure 6A and 6D). The autocorrelations are single-exponential with decay time constants of 1.39 ms for C343 (Figure 6C) and 2.67 ms for CV⁺ (inset of Figure 6D). Under ambient conditions, the time scale of the triplet blinking is presumably shorter than 1 ms. Therefore, the millisecond blinking time due to the triplet state is clearly distinguished from the fluorescence intensity fluctuation time of subseconds to seconds. Furthermore, under low-power (<50 W/cm²) laser excitations, the fluorescence fluctuations are mostly spontaneous and do not originate primarily from the photoinduced triplet-state dynamics, which is consistent with the fluorescence fluctuations on the milliseconds-to-seconds time scale.

The nature of the lower fluorescence intensity levels has been further investigated. One possibility is that emission from the oxidized states of the dye molecules (C343⁺ and CV²⁺) may be responsible for lower fluorescence intensity levels. However, it is known in the literature that the oxidized states of the dye molecules (C343⁺ and CV²⁺) produce no fluorescence or extremely weak fluorescence^{28,37} that would not be significant compared to background. A second possibility is the fluorescence quenching by the ET process. The time scale of the FET processes are known to be from femtoseconds to subnanoseconds,^{16,18–20,23,24,28,29,36,42–46,48} while the fluorescence lifetimes of C343 and CV⁺ are in nanoseconds.^{22,24,28,34,35,37,44} Based on the rates of FET and fluorescence, extremely low fluorescence quantum efficiency is expected.

It is an apparent paradox that single-molecule fluorescence is observed along with ET processes. We investigated this intriguing observation by analyzing the fluorescence lifetimes of single molecules. In this experiment, the arrival and delay times of every detected photons were recorded using the time-stamping technique.⁷⁵ The arrival time was used to construct

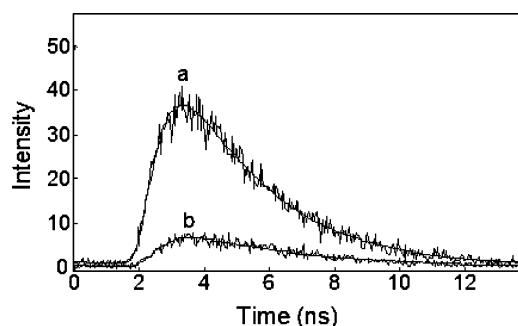


Figure 7. Fluorescence decay profiles of a single CV⁺ molecule, whose intensity trajectory is provided in Figure 4D. The trajectory (Figure 4D) is separated into higher and lower levels based on a photocount threshold of 30 per 10 ms: Traces a and b are the nanosecond fluorescence decay curves of the photons emitted within the higher and lower intensity periods, respectively. The curves are fitted to single exponential decays with time constants of 2.6 ns (a) and 3.4 ns (b). Both the curves are normalized based on their total accumulation time. The ratio of the pre-exponential amplitudes of the higher and the lower intensity curves is 6.

an intensity trajectory and the delay time to analyze single-molecule fluorescence lifetimes. Figure 4D shows the intensity trajectory of a typical single CV⁺ molecule constructed from the photon arrival time. The photon delay time of the same single molecule can be used to derive the fluorescence lifetime correlated to the intensity trajectory. For this, the trajectory was separated into higher and lower levels, based on a photon count threshold of 30 per 10 ms. Then, the nanosecond fluorescence decay curves were plotted, based on the delay time of photons in each group (Figure 7). The curves were fitted to single exponential decays with time constants of 2.6 ns (for profile a in Figure 7) and 3.4 ns (for profile b in Figure 7). We found that the fluorescence lifetimes of the higher and the lower intensity states are very close for the molecule shown in Figure 7. However, the pre-exponential amplitude of the higher intensity state is 6 times higher than that of the lower. Therefore, the intensity difference between the profiles (traces a and b in Figure 7) is attributed to the difference in the pre-exponential amplitudes. On the other hand, quenching of the singlet excited state due to interfacial ET reactions occurs at hundreds of picoseconds or below and is much faster than our instrument response time. The observed time scale of this fast quenching process of single molecules agrees with the reported fast FET rates in general. Similar behavior is observed in the analyses of the intensity trajectories of other single molecules. Nevertheless, the single molecules still show reasonable fluorescence intensity, likely because the ET process dominates the fluorescence process only a fraction of the time. The fluorescence intensity level is determined by the fraction of time during which the intermittent ET process takes place but not by the rates of ultrafast ET reactions. The fluctuations in the fluorescence intensity trajectories are due to high and low ET reactivities of the single C343 and CV⁺ molecules with TiO₂ NPs. Both lower and higher intensity states have a distribution; i.e., they are not discrete states (for example, Figure 4). It is unlikely that interfacial electron transfer processes are completely turned “on” and “off” during the periods of the lower and higher fluorescence intensity states, respectively. On the other hand, each lower and higher intensity state likely includes occurrences of multiple FET and BET events. Therefore, only the time-binning-averaged intensities were recorded in the single-molecule trajectories. The fluorescence intensity fluctuations reflect that interfacial electron

transfer reactivity changes from time to time stochastically, resulting in different time spans of the lower and higher intensity states. When the interfacial ET reactivity is high, the ultrafast redox reactions dictate the fate of the singlet excited state of the dye molecules, and the fluorescence quantum efficiency is low or close to zero. In contrast, when the redox reactivity is low or nonexistent, the fluorescence quantum efficiency is high, and so is the fluorescence intensity.

It has recently been substantiated that ET processes are responsible for fluorescence blinking on the subsecond-to-several-second time scale of single-molecule electron donor–acceptor systems⁵⁶ and semiconductor-single-molecule electron donor systems.²⁶ The fluorescence intensity of “on” and “off” periods has been interpreted as single redox state turnover events, i.e., the on–off “blinking” time constants are the ET time constants. However, in the dye–TiO₂ systems that we have studied, it is unlikely that such slow ET processes dominate. Extensive ensemble-averaged fluorescence and transient absorption studies of interfacial ET processes have proven that FET and BET processes in interfacial ET systems, such as C343–TiO₂ and CV⁺–TiO₂ systems, take place on the subpicosecond to microsecond time scale. Based on the results of our control experiments, single-molecule experiments, and the literature, we attribute the fluorescence fluctuations and blinking of the dye–TiO₂ systems to the intermittent changes of the single-molecule interfacial ET redox turnover rates, i.e., to reactivity changes rather than to individual redox turnover events. Therefore, rather than specifically identifying FET and BET rates, we are able to observe the intermittent interfacial ET dynamics, which provides new information that can only be obtained from single-molecule experiments.

The single-molecule interfacial ET processes in C343–TiO₂ and CV⁺–TiO₂ systems were found to be inhomogeneous, both dynamically and statically. The static inhomogeneity originates from different interfacial ET reactivity fluctuations from molecule to molecule, whereas dynamic inhomogeneity is associated with the ET reactivity fluctuations from time to time for the same individual molecules, resulting in fluorescence fluctuations. Based on extensive literature on ensemble-averaged ET dynamics and mechanisms, we attribute the origins of these static and dynamic inhomogeneities in the single-molecule interfacial ET processes to fluctuation of the molecular properties, including donor–acceptor distance, redox potentials of the donor and the acceptor, Franck–Condon factors, donor–acceptor electronic coupling, and the solvent reorganization energy.^{38,39,50–53,85–87} Among these critical parameters, the changes in Franck–Condon coupling^{51–53,85–87} and associated nuclear motions^{38,39} are most likely to determine the ET rate fluctuation of a single molecule, assuming that other parameters do not change considerably for a single molecule over time. However, limited by the sensitivity of the single-molecule fluorescence spectroscopy, we are not yet able to detect the changes of these parameters. Since the large-scale rotational and translational diffusions are not responsible (Figure 5) for the interfacial ET intermittency of single molecules, we postulate two possible origins: the changes in molecule–surface vibronic coupling due to nuclear motions and the changes in Franck–Condon coupling due to fluctuations of the energy gap between

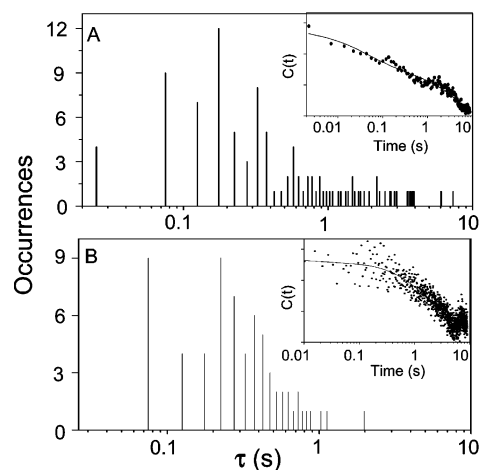


Figure 8. Histograms of fluorescence intermittency time constants, obtained from intensity trajectory autocorrelations, for >100 single molecules of C343 (A) and CV⁺ (B) adsorbed on TiO₂ NP surfaces. The insets in parts A and B are typical fluorescence intensity trajectory autocorrelation traces for single C343 and CV⁺ molecules, respectively.

the reactants and products.^{38,39,85–87} We observed the dynamic inhomogeneity of the interfacial ET reactions by obtaining and analyzing autocorrelation functions (insets of Figure 8A and B) of single-molecule fluorescence intensity fluctuations and blinking. The autocorrelation decays are typically nonexponential and fitted using biexponential decays, with the decay times ranging from 10 ms to 30 s. The nonexponential and power-law behavior^{70–72} of the autocorrelation function decays, which stretched across wide time scales, from sub-milliseconds to minutes, shows the dynamic inhomogeneity of the single-molecule interfacial ET reactivities. The cutoff at sub-milliseconds of the power-law decay was due to our measurement system response limitation. It is highly likely that the dynamic inhomogeneity extends to shorter time scales.

Using autocorrelation function analyses of the fluorescence intensity trajectories, we observed that the interfacial ET reactivities of both the C343 and CV⁺ single molecules are statically inhomogeneous, varying the rate of the ET reactivity fluctuations from molecule to molecule and from site to site for C343 and CV⁺ molecules adsorbed on the surface of TiO₂ NPs. We obtained broad distributions of the nonexponential intensity autocorrelation decays for C343 and CV⁺ single molecules (Figure 8A and 8B), strongly suggesting that the ET systems are statically inhomogeneous. We note that our measurements were only able to probe a portion of the intermittency dynamics, due to limited time resolution and single-molecule photobleaching. Although the statistical significance of the difference between the autocorrelation time distributions of the two systems was not large, the slightly narrower distribution of CV⁺ compared to that of C343 in the ET-induced fluorescence fluctuation characteristics was probably introduced by the different charge densities, the different interfacial electronic and Franck–Condon coupling efficiencies of C343 and CV⁺ on TiO₂ NPs, and the differences in the local nanoscale environments of individual molecules, e.g., surface roughness, vacancies, etc.. The changes in the coupling of the dye molecules with the electron-accepting TiO₂ surface were mostly spontaneous, since we used low laser excitation power, and demonstrated that the fluctuation is not dominated by the photoinduced triplet-state process (Figure 4). The single-

(85) Hupp, J. T.; Williams, R. D. *Acc. Chem. Res.* **2001**, *34*, 808–817.

(86) Parson, W. W.; Warshel, A. *Chem. Phys.* **2004**, *296*, 201–216.

(87) Warshel, A.; Parson, W. W. *Annu. Rev. Phys. Chem.* **1991**, *42*, 279–309.

molecule interfacial ET reactivity shows intrinsic static and dynamic inhomogeneities, which would be extremely difficult to identify and characterize by conventional ensemble-averaged measurements.

Conclusion

Applying single-molecule fluorescence spectroscopy and time-correlated single-photon counting, we observed intermittent interfacial ET of single dye molecules adsorbed on TiO₂ NP surfaces. The intermittent interfacial ET dynamics were found to be inhomogeneous, involving different rates, among the single molecules. Autocorrelation function analyses of the single-molecule fluorescence intensity trajectories revealed that kinetics of the intermittent interfacial ET reactivities exhibit nonexponential behavior. The intermittent interfacial ET dynamics originated from the interruption and perturbation of the couplings between the adsorbed dye molecules and the TiO₂ surfaces. We

postulate that intermittent dynamics are common for the interfacial chemical reactions that involve interaction between adsorbed molecules and substrate surfaces. The spontaneous thermal motions of the molecules occur on a wide time scale, particularly at room temperature, introducing perturbation into the rate-determining interactions between molecules and substrates, which, in turn, results in the interfacial ET reaction-rate fluctuation and intermittency. At this time, using single-molecule fluorescence spectroscopy, we are unable to identify and quantitatively characterize the molecular properties that control the ET processes, including the donor–acceptor electronic coupling, the redox reaction driving force,⁸⁸ the Franck–Condon factor, and the nuclear relaxation energies. Single-molecule Raman might enable such a quantitative identification, although significant technical challenges exist for a Raman study of single-molecule interfacial ET dynamics.^{9,89,90}

Acknowledgment. We thank Steve Colson for helpful discussions and Chongmin Wang for help on the TEM measurements. This work was supported by the Office of Basic Energy Sciences within the Office of Science of the U.S. Department of Energy (DOE). The Pacific Northwest National Laboratory is operated by Battelle Memorial Institute for DOE under Contract DE-AC06-76RLO1830.

JA040057B

(88) We have explored the ET driving force dependent experiments by applying a bias voltage across the TiO₂ NPs–electrolyte interface. A multilayer of TiO₂ NPs was spin-coated on an indium tin oxide (ITO) coated glass plate, and then single C343 or CV⁺ molecules are deposited on the TiO₂ NP layer, followed by connecting the TiO₂ coated surface to the working electrode of a potentiostat (CV27 potentiostat, Bioanalytical Systems, Inc.) and dipping a silver wire into the electrolyte as a reference electrode. We examined single-molecule fluorescence behavior in this system under applied bias voltage in the range -2 V to $+2$ V. However, we were unable to draw a definitive conclusion on the single-molecule driving-force dependent interfacial ET dynamics based on our preliminary results from the potential controlled experiments, limited by the various complexities associated with the systems, such as inhomogeneous potential distributions in the semiconductor and at the semiconductor–electrolyte interfaces due to the roughness of the TiO₂ NP surfaces, nanoscale gradient dielectric constants and electric conductivity, inhomogeneous surface electric work functions, etc..

(89) Jiang, J.; Bosnick, K.; Maillard, M.; Brus, L. *J. Phys. Chem. B* **2003**, *107*, 9964–9972.

(90) Rossetti, R.; Brus, L. E. *J. Am. Chem. Soc.* **1984**, *106*, 4336–4340.